Journal of Structural Geology 32 (2010) 1923–1932

Contents lists available at ScienceDirect

Journal of Structural Geology

journal homepage: www.elsevier.com/locate/jsg

Chemical diagenetic constraints on the timing of cataclasis in deformed sandstone along the Pine Mountain overthrust, eastern Kentucky

Astrid Makowitz [a], Robert H. Lander [b], Kitty L. Milliken [c,*]

[a] Cimarex Energy Company, 1700 Lincoln St. Suite 1800, Denver, CO 80203-4518, USA
[b] Geocosm, LLC, 3311 San Mateo Drive, Austin, TX 78738, USA
[c] Bureau of Economic Geology, Jackson School of Geosciences, The University of Texas at Austin, 10100 Burnet Road, Austin, TX 78713, USA

ARTICLE INFO

Article history:
Received 7 August 2009
Received in revised form
3 April 2010
Accepted 26 April 2010
Available online 5 May 2010

ABSTRACT

Cathodoluminescence imaging reveals that sandstones of the middle Pennsylvanian Lee Formation and Breathitt Group along the Pine Mountain Overthrust (PMO) contain inter- and intra-granular authigenic quartz in proportions that differ markedly between samples of contrasting deformational state. Fracture surfaces generated during fault movement provided nucleation substrates favorable for the emplacement of substantial amounts of intragranular quartz (up to 11 volume percent in the Lee Formation). Relatively undeformed sandstones contain cement that is dominantly intergranular whereas sandstones from highly deformed cataclasites along the trace of the PMO contain cement that is dominantly localized within intragranular fractures. Therefore, the chemical diagenetic histories of different samples of Breathitt and Lee sandstones diverged markedly as a consequence of differing deformational histories and the cementation history thus constitutes a record that is relevant to deciphering the timing of deformation.

The small quantities of early-formed, intergranular cement within the cataclasites (average 3.7 volume percent), show evidence of breakage and accordingly, must have largely pre-dated the deformation. Quartz cementation modeling (Touchstone™) suggests that emplacement of this pre-deformational intergranular cement within these deformed rocks can be bracketed within a period from approximately 280 to 260 Ma. An interpretation of fault movement that shortly post-dates this initial period of quartz cementation is consistent with other estimates for the timing of the Alleghanian orogeny. Because of their protracted period of burial, rocks in the vicinity of the PMO remained at temperatures amenable to continued quartz cementation until the middle Cenozoic, and thus, most of the quartz cementation in the cataclasites and also in the surrounding undeformed sandstones post-dates movement on the fault.

1. Introduction

Deciphering the way in which chemical and mechanical processes operate in concert is vital for understanding the evolution of rock properties (both chemical and mechanical). For example, brittle processes such as compactional grain crushing and through-going fracturing impact chemical processes such as cementation by dramatically changing the availability of essential nucleation substrates (Chuhan et al., 2002; Makowitz and Milliken, 2003; Laubach et al., 2004; Makowitz, 2004; Milliken et al., 2005), thus affecting the ultimate volume and spatial distribution of cement (Bloch et al., 2002; Makowitz and Milliken, 2003; Milliken et al., 2005; Eichhubl et al., in press) and even the rates of cement emplacement (Lander et al., 2008). In turn, emplacement of cement induces lithification that profoundly impacts the mechanical properties of granular aggregates (Dvorkin et al., 1991, 1994; Bernabé and Brace, 1992; Zang and Wong, 1995; Elata and Dvorkin, 1996; Dewhurst and Jones, 2003; Laubach and Ward, 2006; Olson et al., 2007).

Several authigenic minerals display precipitation-rate behavior that can be described using empirically-determined Arrhenius kinetics (Walderhaug, 1994b, 1996; Lander and Walderhaug, 1999; Perez and Boles, 2005; Lander et al., 2008). Thus, the observed volumes of these cements can provide an estimate of the timing and conditions of cement precipitation when such kinetic models are used in concert with reconstructed thermal histories (Makowitz et al., 2006). If the paragenesis of such cements can be placed in the context of a deformational event or process (e.g., Laubach and Diaz-

* Corresponding author. Tel.: +1 512 471 6082; fax: +1 512 471 0140.
E-mail address: kittym@mail.utexas.edu (K.L. Milliken).

0191-8141/$ – see front matter © 2010 Elsevier Ltd. All rights reserved.
doi:10.1016/j.jsg.2010.04.014

Tushman, 2009; Becker et al., 2010), the quantitative estimates of timing that arise from the modeling of cement emplacement can then be applied to the deformation as well.

This study uses empirical-kinetic modeling of quartz cement precipitation in middle Pennsylvanian sandstones and associated fault rocks to obtain constraints on the timing of the Pine Mountain Overthrust (PMO), a classic and well-documented example of thrust-faulting along the eastern side of the Southern Appalachian foreland basin.

2. Geologic setting

The complex history of the Appalachian Basin foreland basin involves a multi-stage history that includes Taconic (450 Ma, Ordovician), Acadian (410–380 Ma, Devonian), and Alleghenian (320–260 Ma, Carboniferous) thrusting episodes (Quinlan and Beaumont, 1984; Tankard, 1986; Beaumont et al., 1987). The Alleghanian Orogeny is the most important deformation event in terms of its strong overprint on the depositional style and structure of the region.

The PMO is the western-most Alleghenian-age structure in the southern Appalachians, crossing Virginia, Tennessee, and Kentucky (Fig. 1) and is considered to be a classic example of the structural style in fold and thrust belts adjacent to foreland basins (Wilson and Stearns, 1958; Miller, 1962; Zafar and Wilson, 1978; Mitra, 1988). The fault disrupts the orogenically-derived clastic sediments of the Lee Formation and Breathitt Group, and thus must post-date the middle-Pennsylvanian. The structural geometry consists of an east-northeast striking major thrust that climbs from a detachment in the Cambrian Rome Formation through successively younger units and flattens into a detachment localized in the Devonian Chattanooga Formation wherein it reaches the surface (Zafar and Wilson, 1978; Mitra, 1988). The surface exposure of the thrust sheet consists of a rectangular block about 200 km long and 40 km wide, bounded on the northwest by the Pine Mountain Fault, to the southeast by the Wallen Valley and Hunter Valley faults (Mitra, 1988). The thrust sheet terminates to the southwest and northeast at two primary tear faults, the Jacksboro and the Russell Fork Faults, respectively. Total displacement associated with the PMO system decreases from about 21.3 km at the southwestern end to less than 3 km on the northeastern end (Mitra, 1988). All along

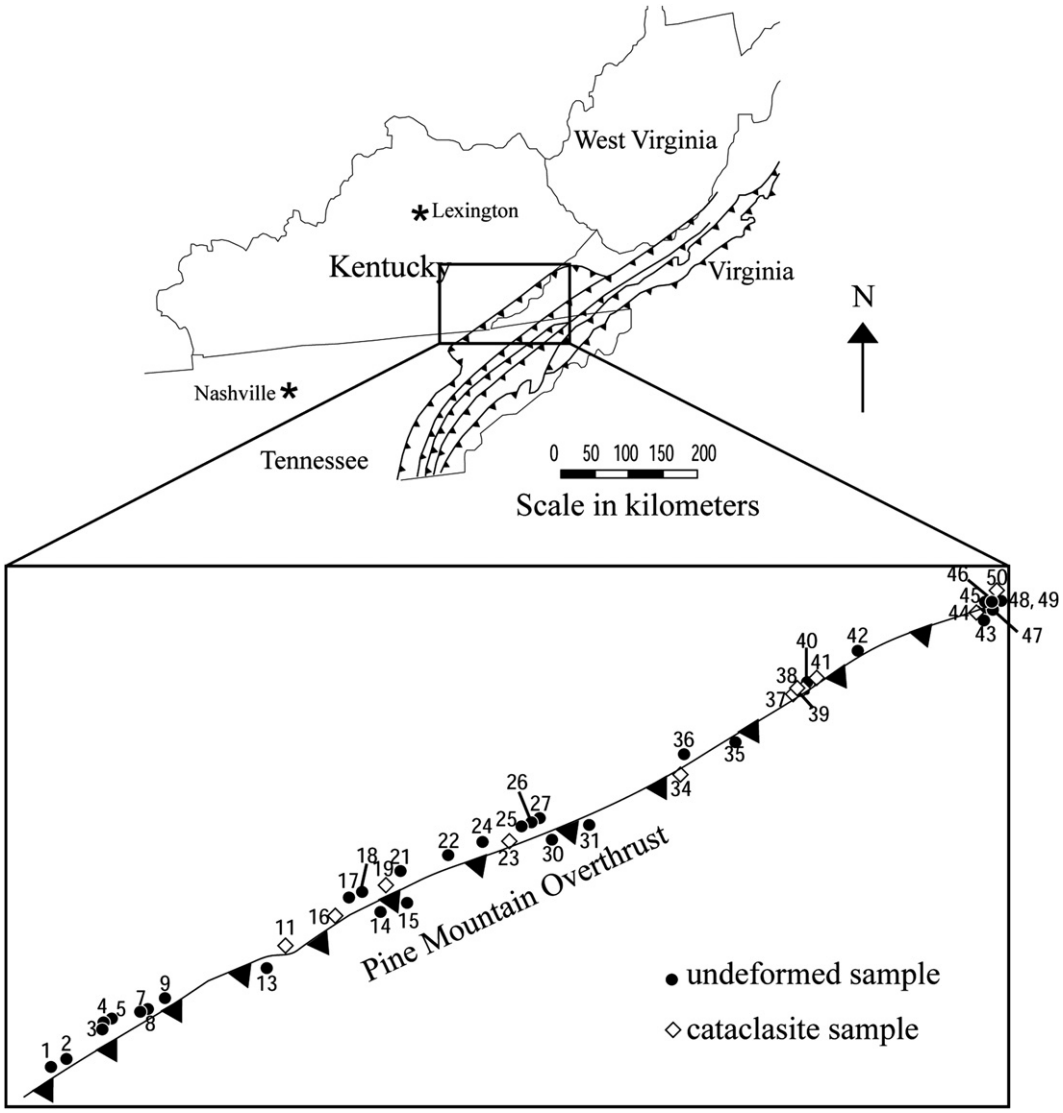

Fig. 1. Study area and sampling locations.

the trace of the fault, the Breathitt and Lee sandstones immediately in front of and below the PMO are highly deformed and locally overturned. In addition, at several localities complex second- and third-order thrusts form slices that climb from the main detachment into the overlying Pennsylvanian units (e.g., Froelich, 1972; Froelich and Tazelaar, 1973, 1974)

The thickness and maximum burial of the Carboniferous rocks deposited in the southern Appalachian Basin increase towards the orogen and the PMO (Johnsson, 1986; O'Hara et al., 1990; Roden, 1990; Hower and Rimmer, 1991). Consistent with this, the Pennsylvanian sandstone above the PMO (initially deposited in the more rapidly subsiding part of the basin) generally display diagenetic features such as greater compaction and quartz cementation consistent with greater burial and thermal exposure (Milliken, 1998). Based up on apatite fission track analysis (AFTA), maximum temperatures experienced by the northern PMO exceeded 110 °C and a burial depth of 3 km (Boettcher and Milliken, 1994). This estimate from AFTA is in broad agreement with estimates from coal maturation studies by O'Hara et al. (1990) of 2.9–3.1 km maximum burial of the Fire Clay Coal in the vicinity of the PMO. South of the PMO, in southwestern Virginia, Ordovician rocks indicate a maximum burial and maximum temperature of 3.4 km and 120 °C, respectively (Roden, 1990). Data from farther north in the basin (Virginia, West Virginia, and Maryland) from Devonian rocks yield identical values (Roden et al., 1993).

The data of Boettcher and Milliken (1994) indicate that cooling probably commenced in the Jurassic, with temperatures remaining >60 °C until the Late Cretaceous to Miocene. This thermal history is consistent with that proposed (also from AFTA) for southwestern Virginia and southern Pennsylvania (Roden, 1990; Roden et al., 1993) and also with a regional study in the vicinity of the PMO using coal rank trends (for Pennsylvanian coals) (Hower and Rimmer, 1991). The timing of unroofing initiation may be contemporaneous with the transition from rift- to drift-extension along the Atlantic continental margin (Poag, 1992). A final and relatively rapid period of uplift occurred in the Miocene (Blackmer, 1992; Boettcher and Milliken, 1994), an event that is recorded in the thick siliciclastic units of Miocene age on both the Atlantic margin of North America (Poag and Sevon, 1989; Poag, 1992) and in the Gulf of Mexico (Galloway et al., 2000; Galloway, 2005).

The Lower Pennsylvanian Lee Formation and the formations of the middle Pennsylvanian Breathitt Group crop out extensively along the PMO. The Lee Formation is composed of massive, largely quartzose sandstone and the Breathitt Group is the dominant coal-bearing unit of the region and includes lithic sandstone, siltstone, mudstone, coal, and underclay. The Lee Formation is dominantly fluvial whereas the Breathitt group lithologies represent primarily deltaic environments interspersed with marine transgressive mudstones (Greb and Chesnut, 1996). Compositionally, both the Lee and Breathitt sandstones reflect derivation from mixed orogenic sources consistent with their foreland basin setting, including older siliciclastic rocks, carbonate sedimentary rocks, mica-rich metamorphic rocks, crystalline basement, and a very minor component of volcanic or shallow intrusive rocks (Fu et al., 1994; Milliken, 1998, 2001, 2002, 2003; Makowitz, 2004)

3. Sampling

Samples were collected along the entire 200 km length of the thrust (Fig. 1). The fault itself is not well-exposed, but intensely deformed blocks of cataclasite occur discontinuously along and immediately in front of the PMO as pods that range from a few tens

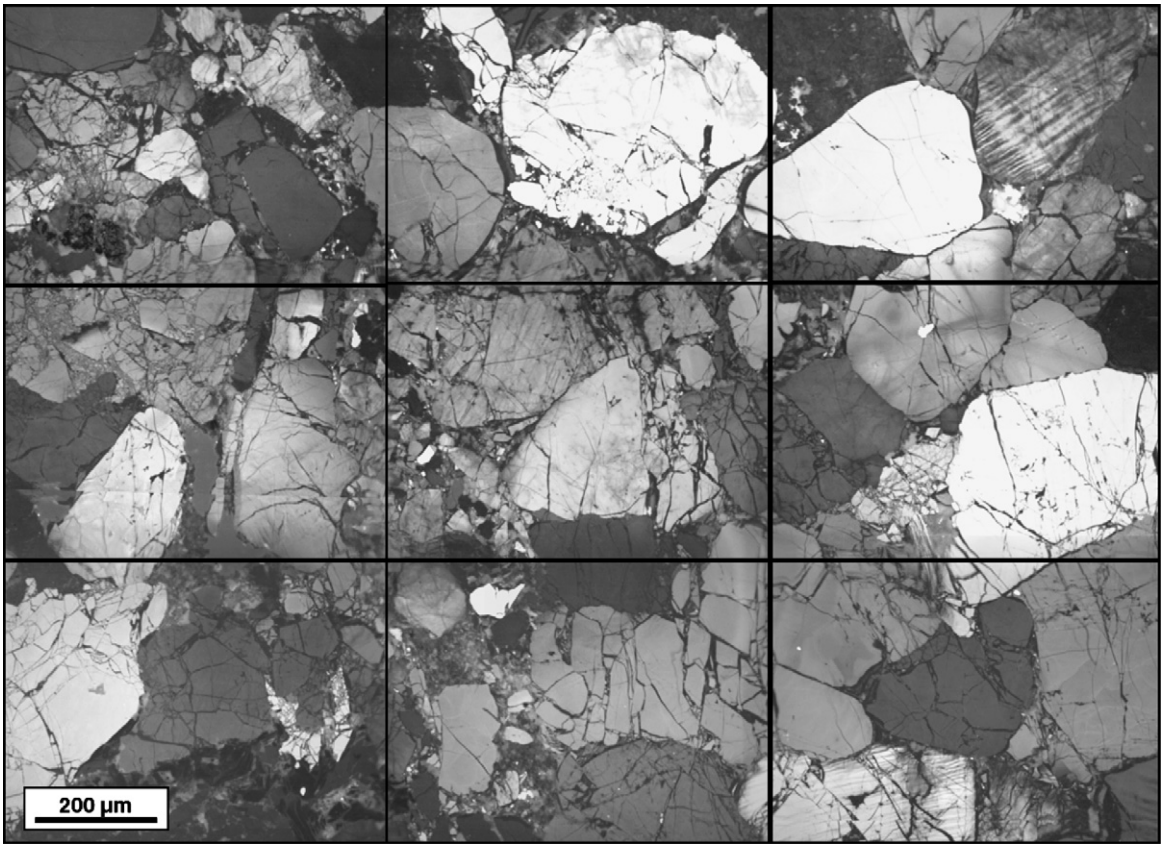

Fig. 2. Mosaic of cathodoluminescence images used to for point-counting the abundance of detrital quartz and quartz cement (inter- and intra-granular).

Table 1
Point-count data.

Sample type/ unit	Sample	Inter-granular quartz cement	Intra-granular quartz cement	Total quartz cement	Intra-granular/ total cement	IGV
Cataclasite samples						
Lee	16	4.8	4.0	8.8	45.7	13.4
	16b	3.5	9.5	13.0	73.3	13.6
	19	6.4	8.2	14.6	56.0	15.5
	34	1.1	9.4	10.5	89.2	12.5
	37	3.2	6.4	9.6	66.5	10.2
	38a	1.6	10.9	12.5	87.0	14.4
	38b	3.0	5.4	8.4	64.6	14.7
	38c	2.5	6.1	8.6	70.9	14.3
	39	3.3	7.9	11.2	70.7	11.3
	41	0.8	7.9	8.7	91.2	9.0
	50	4.4	7.3	11.7	62.5	11.7
	Average	**3.1**	**7.5**	**10.7**	**70.7**	**12.8**
Breathitt	11	5.8	4.0	9.8	40.8	12.3
	23	4.6	3.2	7.8	41.3	11.0
	44	6.8	3.9	10.7	36.8	12.6
	Average	**5.7**	**3.7**	**9.4**	**39.7**	**12.0**
Undeformed samples						
Lee	17	10.5	1.5	12.0	12.5	16.6
	18	12.0	1.0	13.0	7.7	18.6
	42	7.3	3.8	11.1	34.2	12.7
	45	9.7	1.2	10.9	11.0	11.9
	46	10.1	1.1	11.2	9.8	11.9
	47	15.0	1.3	16.3	8.0	17.3
	Average	**10.8**	**1.7**	**12.4**	**13.9**	**14.8**
Breathitt	1	7.4	1.0	8.4	11.9	10.1
	2	9.9	0.2	10.1	2.0	11.6
	3	5.3	3.2	8.5	37.6	12.0
	4	6.2	1.8	8.0	22.5	11.8
	5	15.7	0.7	16.4	4.3	17.4
	7	13.7	0.7	14.4	4.9	18.7
	8	13.7	0.9	14.6	6.2	21.5
	9	18.5	0.8	19.3	4.1	21.0
	13	5.9	2.0	7.9	25.3	12.3
	15	8.1	0.8	8.9	9.0	12.7
	21	6.8	2.0	8.8	22.7	9.0
	22	5.4	1.4	6.8	20.6	6.9
	24	10.6	3.6	14.2	25.4	16.6
	25	14.5	1.9	16.4	11.6	19.9
	26	8.5	1.6	10.1	15.8	19.5
	27	4.6	1.1	5.7	19.3	8.5
	30	10.8	1.9	12.7	15.0	14.4
	31	10.9	1.2	12.1	9.9	13.2
	35	7.5	4.3	11.8	36.4	16.0
	36	6.1	1.2	7.3	16.4	8.1
	40	8.1	1.2	9.3	12.9	9.9
	48	9.5	1.4	10.9	12.8	15.6
	49	12.5	2.8	15.3	18.3	17.2
	51	16.8	0.9	17.7	5.1	18.3
	52	18.9	1.0	19.9	5.0	21.4
	Average	**10.2**	**1.6**	**11.8**	**15.0**	**14.5**

Letters (a, b, c) indicate multiple samples from a single locality, the locality numbers being shown in Fig. 1.

to hundreds of meters in length. Bedding in these pods is nearly undetectable. Faint linear and anastomosing deformation bands can be observed locally, but in general the cataclasites appear to be nearly homogeneous in outcrop. Fourteen cataclasites were collected from 11 outcrops. Eleven of the 14 cataclasite samples are quartz-rich Lee Formation and the remaining 3 have compositions consistent with the lithic-rich Breathitt sandstones. Thirty-one sandstones, not visibly affected by the thrust fault were also collected in close proximity to the fault, of which 6 are from the Lee Formation and 25 from the Breathitt Group. It is important to note that although these "undeformed" samples come from outcrops that have near-to-horizontal bedding and clearly visible sedimentary structures, they are not entirely devoid of deformational effects at the microscale, having many small quartz-filled microcracks and pressure solution features.

4. Petrography

The abundance of detrital grains, cements, and porosity in each of the samples was determined using scanned cathodoluminscence imaging, a powerful tool for discriminating quartz cement from detrital quartz (Sippel, 1968). Uncoated polished thin sections were imaged using a Gatan PanaCL cathodoluminescence detector (with RGB color filters) installed on an FEI XL 30 environmental scanning electron microscope (ESEM). Four non-overlapping areas of approximately 3.4 mm^2 were selected for imaging on each sample by using a random number generator to select the x–y coordinates on the ESEM stage. For each area a collage of 9 images (Fig. 2) was collected and stitched using the image stitching program Panavue™. A grid with 400 intersections was applied to each mosaic and components were recorded at each intersection, yielding a total count of 1600 points per sample. Point-count data are presented in Table 1.

The cataclasite samples and undeformed samples of both Lee and Breathitt sandstones do not show significant contrast in terms of their compactional state (as measured by the intergranular volume), nor in the total quartz cement content (Table 1). Instead, the main contrast lies in the distribution of the quartz cement, the undeformed samples being dominated by intergranular quartz cement whereas the cataclasites contain a substantially higher proportion of intragranular (fracture-filling) quartz cement (Fig. 3).

Quartz cement in both deformed and undeformed samples displays a range of colors in cathodoluminescence, including red, dark-blue, and light-blue. The red-luminescing cement is commonly overgrown by the blue (Fig. 4A). Red cement is not pervasively distributed and cannot be found on all grains. Some fractures are filled with red cement, but most are filled by the dark blue quartz (Fig. 4B). The fracturing of the early red-luminescing intergranular cement and its distribution primarily on the outer surfaces of grains indicates that phase of cementation is pre-kinematic (terminology of Laubach, 1988; Laubach and Milliken, 1996). In some samples fractures filled with dark-blue cement cross-cut fractures filled with the red cement (Fig. 4B). The majority of all cement, both on outer grain surfaces and within intragranular fractures is dark-blue. Light-blue cement is less common and post-dates the dark-blue cement and is rarely observed within fractures.

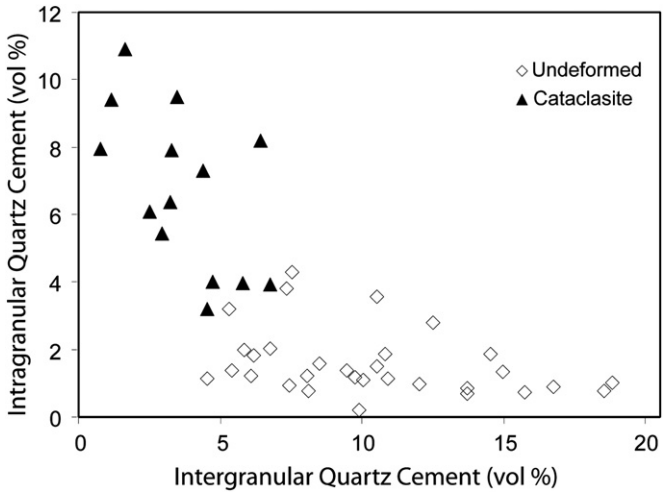

Fig. 3. Quartz cement distribution in cataclasites and relatively undeformed sandstones.

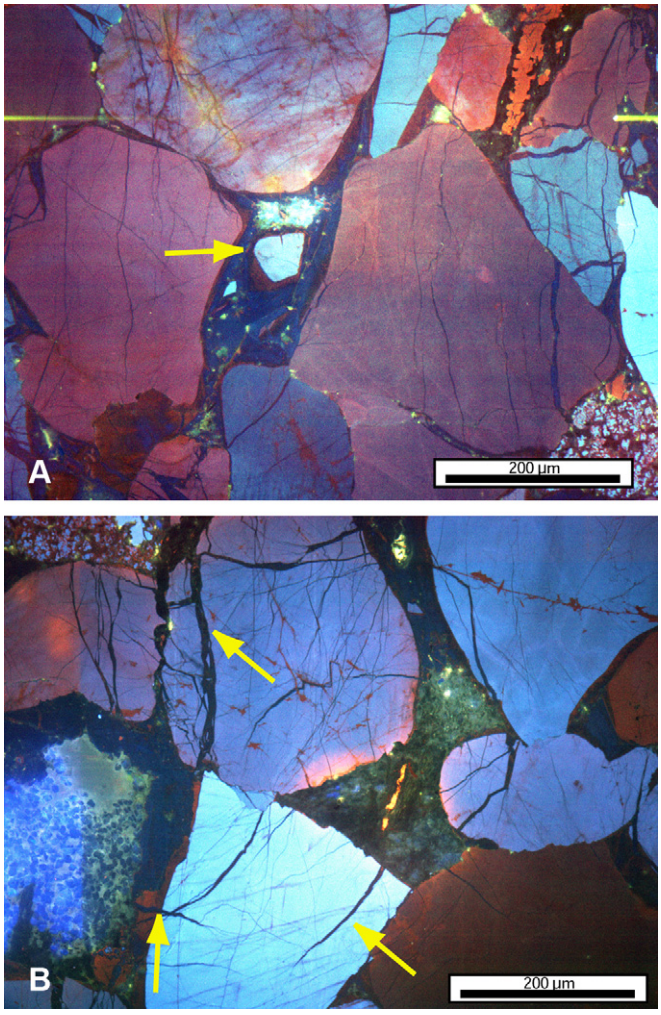

Fig. 4. Cathodoluminescence image showing the varieties and small-scale distribution of quartz cement in PMO cataclasites. A. Cataclasite sample showing thin rims of red-luminescing quartz followed by a larger quantity of blue-luminescing quartz that completely fills the pore. B. Cataclasite sample showing instances of blue fracture-filling quartz cross-cutting the earlier-formed red-luminescing quartz.

5. Modeling approach

An average of approximately 4 volume percent intergranular quartz cement is observed within the deformed samples, ranging from 0.8 to 6.8 percent (Tables 1 and 2). Because the red-luminescing, dominantly intergranular cement pre-dates deformation, the time required to precipitate the observed volumes of this cement within the cataclasites can be used as a constraint on the timing of the deformation. Deformation must therefore post-date the emplacement of this earliest phase of cementation.

It is important to note that CL color and the cross-cutting paragenetic relationships amongst different generations of quartz cement are not being used to here in the quantitative determination of the pre- and post-kinematic cements. Rather, these petrographic relationships are used to confirm that a small portion of the cement is indeed pre-kinematic. The volumetric amounts of the pre-kinematic cement within the cataclasites are measured by virtue of the quantity of intergranular cement in these rocks and it is these values that are used in the modeling. As grains were comminuted the available intergranular space for quartz cement emplacement was diminished, in essence traded, for intragranular spaces which became the dominant loci of quartz precipitation in the deformed rocks. Both deformed and undeformed rocks contain both pre- and post-kinematic cement and the post-kinematic cement is dominant in both sample types.

Table 2
Summary of modeling results.

Quartz cement	Measured	Slow kinetics			Fast kinetics		
		Time, Ma	Temp, °C	Depth, m	Time, Ma	Temp, °C	Depth, m
Average	3.7	261	131	2567	274	96	1817
Min	0.8	270	105	1999	282	66	1270
Max	6.8	259	136	2675	272	102	1940
Range		11	31	676	10.0	36	670

Over the past decade, refinement of a chemical rate model for quartz cementation has provided a means to predict the progress of quartz cementation in the subsurface with considerable accuracy (Lander and Walderhaug, 1999). This model has significant implications for understanding the interrelationships between chemical diagenesis and mechanical rock properties that arise as cement is added progressively to the rock over a period that may coincide with deformation (Olson et al., 2009). The primary controls on quartz cement abundances for "normal" overgrowths in sandstones (i.e., overgrowths related to direct precipitation of quartz from aqueous solution during deep burial and not to silica-precipitating soils or to conversion of opaline silica) are temperature, time, nucleation surface area, and the size of the nucleation substrate (Heald and Renton, 1966; Walderhaug, 1994a, 1996; Lander and Walderhaug, 1999; Walderhaug et al., 2000; Makowitz and Sibley, 2001; Lander et al., 2008; Olson et al., 2009). Quartz precipitation is modeled using an Arrhenius expression that results in an exponential rate increase with temperature (Walderhaug, 2000). The overall nucleation surface area for quartz overgrowths is a function of the abundance and size distribution of detrital quartz grains. Nucleation area, however, declines in the presence of grain coatings (Heald and Larese, 1974) and in association with porosity loss (Lander and Walderhaug 1999; Lander et al., 2008). Cement abundances increase at a somewhat lower than linear rate with time for a given temperature due to (1) a tendency for nucleation surface area to decline with porosity loss and, (2) to an increase in the fraction of the nucleation area associated with slow growing euhedral faces with crystal growth (Lander et al., 2008). Smaller crystal domains tend to have slower rates of growth compared to larger counterparts due to more rapid development of euhedral crystal forms (Lander et al., 2008).

In this study we used the Touchstone™ sandstone diagenesis model (version 7.0 developed by Geocosm LLC) to simulate the pre-deformation history of quartz cementation. This model considers the controls on quartz cementation discussed above as described in greater detail by Lander et al. (2008). Typically this modeling approach employs kinetic parameters that are optimized to match quartz cement abundances from natural sandstones in light of their reconstructed thermal histories. The pervasive quartz cementation and high thermal exposures of the study samples, however, make it difficult to obtain kinetic parameters specifically for the PMO samples because an upper limit cannot be placed on the precipitation rates. Consequently we instead use end-member scenarios in kinetic parameters reported by Lander et al. (2008) to explore a range in the likely time for the onset of cataclastic deformation. These end-member scenarios are derived from geologic settings in which kinetic parameters could be determined from sandstone samples with free surfaces where overgrowths could continue to nucleate and grow. The "fast" kinetics scenario is derived from fluvial sandstones of Miocene age from offshore Southeast Asia whereas the "slow" kinetics scenario corresponds to Ordovician

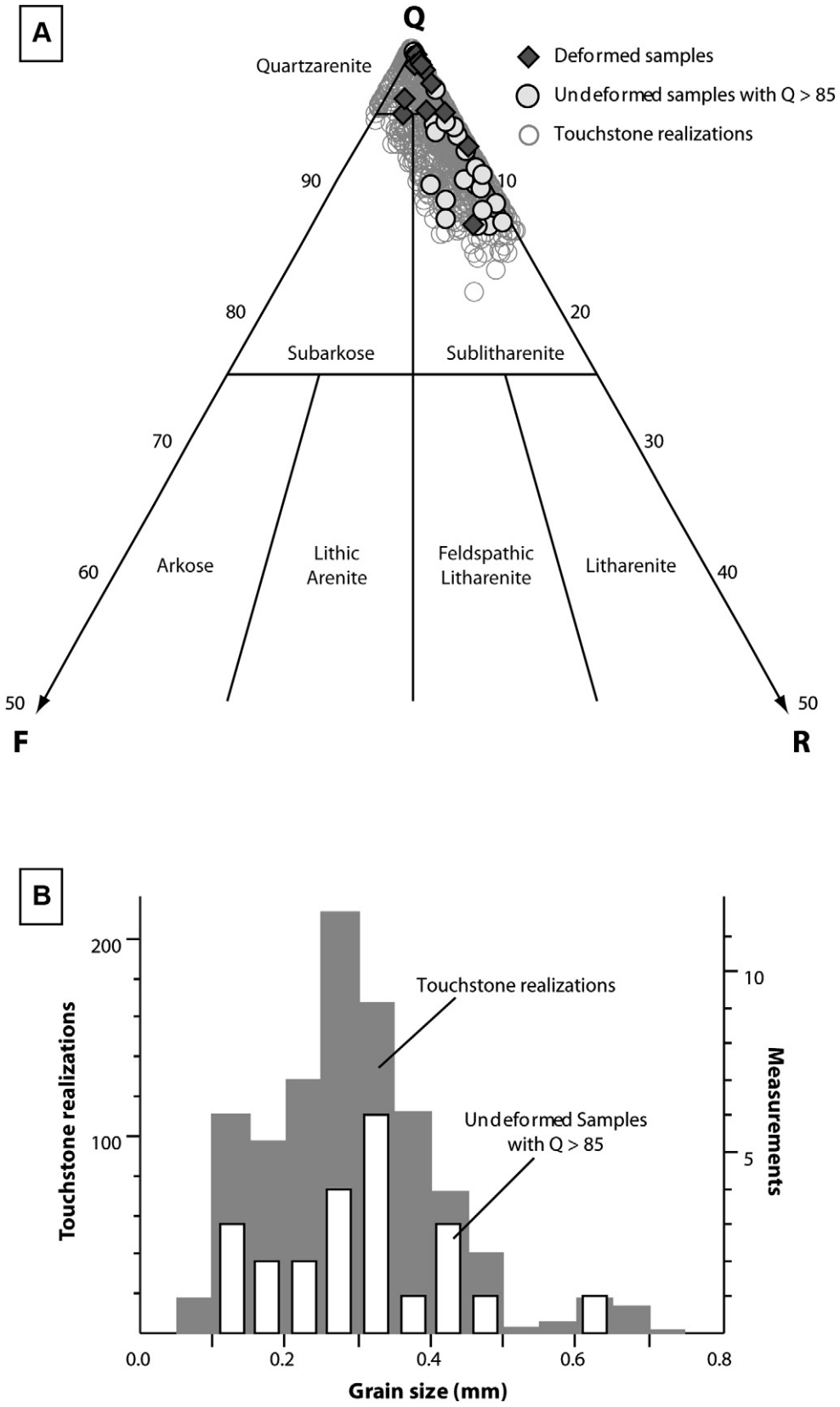

Fig. 5. Comparison of sandstone texture and composition for study samples with Touchstone input realizations. A. Framework grain abundances as shown on the upper half of a QFR diagram (Folk, 1980) for (1) samples with cataclastic deformation, (2) non-cataclastically deformed samples where quartz makes up >85% of the framework grain abundance, and (3) realizations used as input for Touchstone simulations. B. Distributions in mean grain sizes for realizations used as input for Touchstone simulations and non-cataclastically deformed samples where quartz makes up >85% of the framework grain abundance.

samples from a cratonic basin in North America that also was studied by Makowitz et al. (2006). The activation energies for quartz growth for a reference grain size of 0.35 mm for these scenarios are 55.51 and 61.67 kJ/mol, respectively. Both model scenarios use a pre-exponential constant value of $9x10^{-12}$ mol/cm^{2}s and assume the same relative change in growth rate with the size of the nucleation domain.

Because our objective is to reconstruct the pre-deformation history of quartz cementation in the cataclastically deformed samples, the Touchstone simulations employ compositions and grain size distributions that reflect the probable state of the sandstones *prior* to cataclastic deformation. Thus, the non-cataclastically deformed ("undeformed") samples serve as ideal constraints on these sandstone characteristics. Some of the compositions of these samples, however, are significantly less quartzose than their cataclastically deformed counterparts. This compositional difference mainly reflects a larger proportion of samples from the more quartzose Lee Formation in the cataclastically deformed sample set compared to the "undeformed" sample set. In the least quartzose of the cataclastically deformed samples, roughly 85% of the grain volume is made of quartz. We therefore used this compositional cutoff as the basis for identifying analog samples among the "undeformed" samples sample set (Fig. 5A). The resulting analog suite consists of 23 samples.

Our quartz cement results are based on 1000 Touchstone realizations that honor the textures and compositions of the analog samples. We used non-parametric probability distributions to describe variations in framework grain and non-quartz cement abundances as well as in mean grain size, sorting, and grain coating. We also determined Kendal rank correlation coefficients among these sample characteristics and found that the only significant co-variation affecting the pre-deformation characteristics of the sandstones is between quartz grains and phyllite grains (−0.478). We then generated the Touchstone input realizations using a Latin hypercube sampling approach with a bivariate Gaussian copula that accounts for the quartz/phyllite co-variation. These realizations honor the characteristics of the 23 analog samples while representing additional likely compositional and textural combinations for the broader sandstone population. The resulting framework grain proportions for the Touchstone realizations are shown in Fig. 5A. The pre-deformation distribution in mean grain size for the Touchstone realizations is shown in Fig. 5B together with the distribution from the analog samples.

We assume in our simulations that prior to fault movement there was no compaction beyond what occurs under normal burial conditions. The depositional intergranular porosity for all realizations is 45% and is consistent with measured values from fluvial and beach sands (Atkins and McBride, 1992). We defined parameters for Touchstone's compaction model that lead to intergranular volumes (IGVs) ranging from 22 to 28 volume percent at an effective stress of 28 MPa (roughly equivalent to a value expected at 2500 m of burial under hydrostatic fluid pressure and dominantly vertical loading) (Fig. 6). These results are consistent with observations from rigid grain sandstones in basins where vertical loading is the dominant control on effective stress (e.g., (McBride et al., 1991; Lander and Walderhaug, 1999; Paxton et al., 2002). Variations in simulated IGVs reflect differences in the modeled mechanical strength of the sandstone associated with variations in the relative abundances of the framework grains as well as in simulated quartz cement volume. While the simulated IGVs are substantially higher than the measured values for the "undeformed" samples, they are likely to be consistent with the states of these samples prior to faulting. Much of the syn and post faulting IGV loss is due to grain-to-grain chemical compaction ("pressure solution") and brittle grain deformation that occurred at higher stresses and temperatures associated with faulting and subsequent burial.

The other critical input for the simulation is the burial history reconstruction for the sandstone samples along the fault. Genesis™ (developed by Zetaware Inc.) was used to model the thermal and effective stress history. Parameters such as heat flow, types of sediment, and thermal conductivity were taken directly from Rowan et al's. (2004) basin modeling work on the Appalachian region. Maximum burial depth and temperature as well as the unroofing history were taken from studies around or in close proximity to the PMO (Boettcher and Milliken, 1994; Roden, 1990). Basement heat flow is constant through time at 60 mW/m^2 (Rowan et al., 2004). The Breathitt Group and Lee Formation reached a maximum burial during Early Cretaceous time of 5.2 km at 160 °C (assuming a 25 °C/km geothermal gradient). Boettcher and Milliken (1994) document three episodes of varying rates of uplift from AFTA which are used in this study: 1) uplift of 2.3 km of strata from 145 to 80 Ma; 2) 0.4 km removal of strata from 80 to 20 Ma; 3) 1.5 km of strata removal from 20 Ma to the present. All strata uplifted and removed are assumed to be Pennsylvanian and Permian in age composed of a mixture of predominantly sandstones, with some siltstones, mudstones and coals, as described in references on the sedimentation and loading history around the PMO. A necessary assumption is that the same burial history can be applied along the entire trace of the PMO. Because the fault strike parallels the basin's depositional strike it is a reasonable assumption that contrasts in burial histories along this strike-parallel transect will at least be less than the potential differences that would apply to transects that parallel the basinal depositional axes.

6. Modeling results

The outcome for modeling using both fast and slow kinetics as described above and the observed range for the abundance of pre-kinematic quartz cement in the cataclasites is presented in Table 2 and Fig. 7. Based on these ranges of input values the emplacement of the pre-kinematic quartz cementation in the PMO cataclasites was attained within a period corresponding to 280–260 Ma.

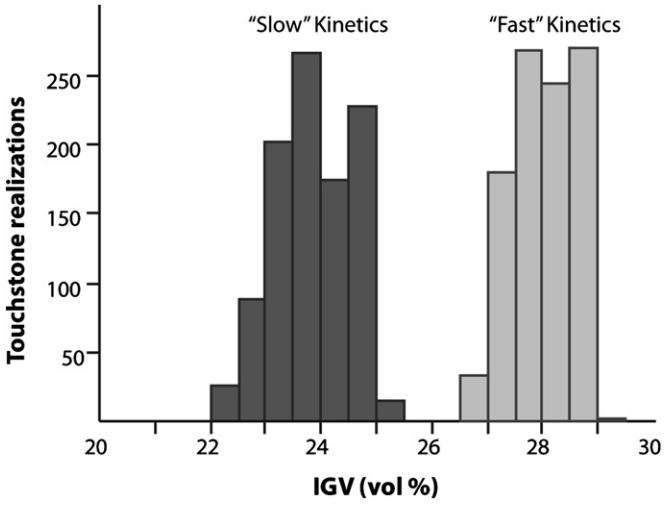

Fig. 6. Modeled intergranular volumes (IGV) at initiation of cataclasis for the two quartz cement kinetic scenarios. IGV values are higher for the "fast" kinetics scenario because rigid quartz cement formed at lower effective stresses associated with shallower depths.

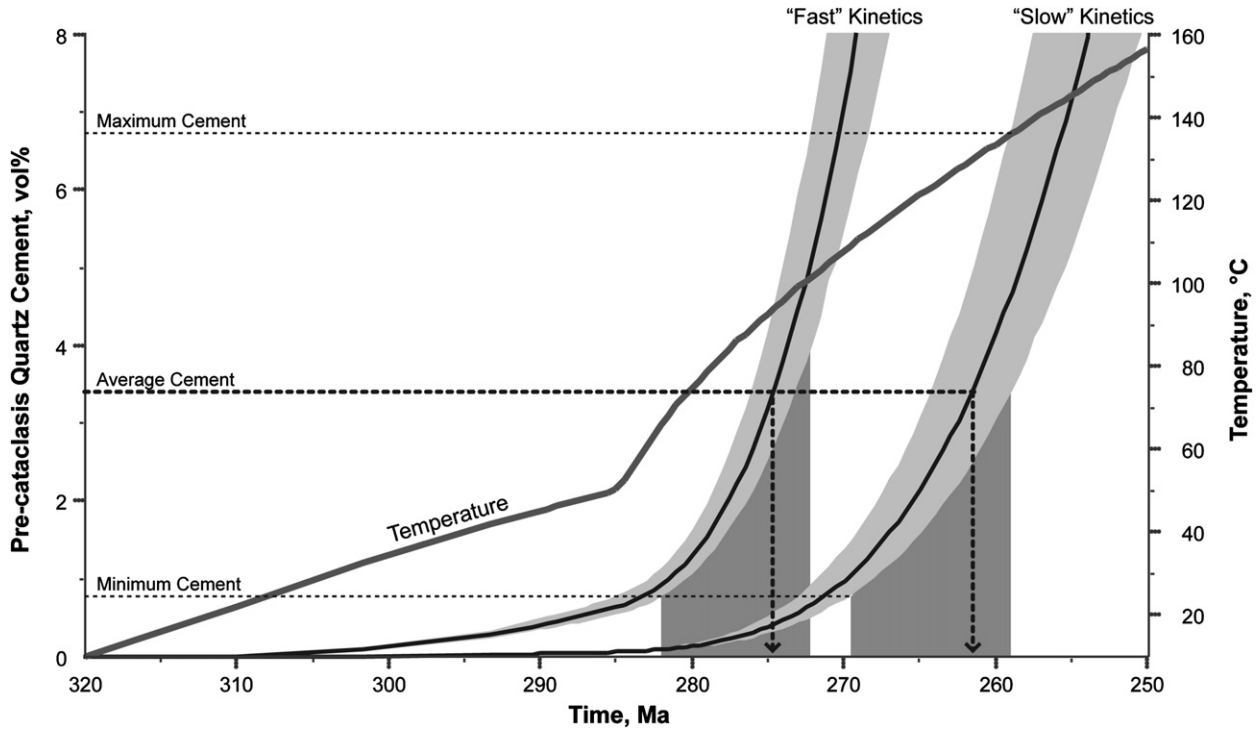

Fig. 7. Timing of quartz cement emplacement for "fast" and "slow" quartz cementation rates across a range of cement contents observed in the cataclasite samples. The light gray envelopes in quartz cement abundance show the calculated range for the 1000 Touchstone realizations whereas the solid central line indicates the average abundance. The dark shaded vertical regions indicate the range in times for completion of the minimum and maximum measured pre-cataclasis quartz cement and the heavy dotted line shows the time when the average measured quartz cement abundance formed.

7. Discussion

No published estimates of timing have been made previously that are specific to movement on the PMO. The faulting is interpreted to entirely post-date deposition (around 310 Ma) given that no growth strata or other evidence of closely syn-tectonic deposition have been described from either the Lee Formation or the Breathitt Group. The regional timing of the Alleghanian in the southern Appalachians has been estimated from the thermal maximum in the Carolina Slate Belt at 295–315 Ma (Secor et al., 1986), followed by

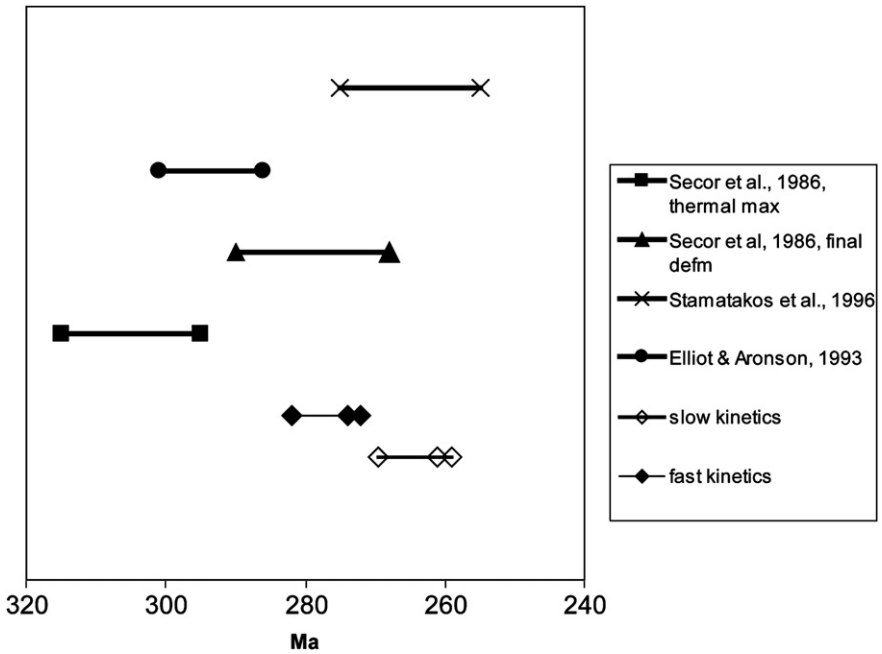

Fig. 8. Comparisons of various estimates for timing of the Alleghanian Orogeny (top 4 bars) with results from this study for the timing of pre-kinematic quartz cementation within cataclasites along the PMO.

episodes of uplift and deformation ending at 268–290 Ma (Secor et al., 1986). Other dates are determined from illitization of bentonites on the Cincinnati Arch at 286–301 Ma (Elliott and Aronson, 1993), remagnetization at 280 Ma (Miller and Kent, 1988), and also remagnetization results for the central Appalachians at 255–275 Ma (Stamatakos et al., 1996). Fig. 8 compares these dates with the constraints for movement on the PMO obtained from quartz cement modeling (~260–280 Ma).

Timing of fault movement interpreted in this study slightly postdates most of the regional estimates, but is still within the overall timing of the Alleghanian orogeny. Timing of Appalachian thrust emplacement is generally regarded to have proceeded from east to west (Hatcher and Odom, 1980) and so, as it represents the western-most of the Alleghanian structures, a relatively young age for the PMO is not surprising.

8. Conclusions

1. In the vicinity of the PMO, the chemical histories of different samples of Breathitt Group and Lee Formation sandstones diverged markedly as a consequence of their contrasting degrees of cataclasis.
2. The abundant fracture surfaces generated during fault movement provided nucleation substrates favorable for the emplacement of substantial amounts of intragranular quartz (up to 11 volume percent in the Lee Formation).
3. Quartz cementation modeling suggests that emplacement of the pre-deformation intergranular cements within the cataclasites was complete by 280–260 Ma, roughly corresponding with published estimates of the timing of the Alleghanian Orogeny. Most of the quartz cement in the cataclasites and also in the undeformed sandstones around the PMO is post-kinematic.
4. The histories of chemical and mechanical processes described here demonstrate the synchronicity of basinal diagenetic and regional structural deformational processes in the sandstones near the PMO.

Acknowledgments

This project was supported by student research grants to AM from the Gulf Coast Association of Geological Societies, the Society for Sedimentary Geology (SEPM), the Geological Society of America, and the Gulf Coast section of SEPM. Support is also acknowledged from the Geology Foundation of the University of Texas and the Fracture Research and Applications Consortium (FRAC) of the Texas Bureau of Economic Geology. Jason and Gordon Gumble braved ticks and poison ivy while helping to collect the samples along the PMO. Zyiong He of Zetaware kindly provided access to the Genesis software. We thank Steve Laubach and Earl McBride for many engaging discussions on structural diagenesis. Publication authorized by the Director, Bureau of Economic Geology.

References

Atkins, J.E., McBride, E.F., 1992. Porosity and packing of Holocene river, dune, and beach sands. American Association of Petroleum Geologists Bulletin 76, 339–355.

Beaumont, C., Quinlan, G.M., Hamilton, J., 1987. The Alleghanian orogeny and its relationship to the evolution of the eastern interior, North America. Memoir 12. In: Beaumont, C., Tankard, A.J. (Eds.), Sedimentary Basins and Basin-forming Mechanisms. Canadian Society of Petroleum Geologists, pp. 425–445.

Becker, S.P., Eichhubl, P., Laubach, S.E., Reed, R.M., Lander, R.H., Bodnar, R.J., 2010. A 48 m.y. history of fracture opening, temperature, and fluid pressure: Cretaceous Travis Peak Formation, East Texas Basin. Geological Society of America Bulletin 122.

Bernabé, Y., Brace, W.F., 1992. The effect of cement on the strength of granular rocks. Geophysical Research Letters 19, 1511–1514.

Blackmer, G.C., 1992. Post-Alleghanian Thermal and Unroofing History of the Appalachian Basin, Pennsylvania.

Bloch, S., Lander, R.H., Bonnell, L., 2002. Anomalously high porosity and permeability in deeply buried sandstone reservoirs: Origin and predictability. American Association of Petroleum Geologists Bulletin 86, 301–328.

Boettcher, S.S., Milliken, K.L., 1994. Mesozoic-Cenozoic unroofing of the southern Appalachian Basin: apatite fission track evidence from middle Pennsylvanian sandstones. Journal of Geology 102, 655–663.

Chuhan, F.A., Kjeldstad, A., Bjørlykke, K., Høeg, K., 2002. Porosity loss in sand by grain crushing–experimental evidence and relevance to reservoir quality. Marine and Petroleum Geology 19, 39–53.

Dewhurst, D.N., Jones, R.M., 2003. Influence of physical and diagenetic processes on fault geomechanics and reactivation. Journal of Geochemical Exploration 2003, 78–79.

Dvorkin, J., Mavko, G., Nur, A., 1991. The effect of cementation on the elastic properties of granular material. Mechanics of Materials 12 (3–4), 207–217.

Dvorkin, J., Nur, A., Yin, H., 1994. Effective properties of cemented granular materials. Mechanics of Materials 18 (4), 351–366.

Eichhubl, P., Hooker, J.N., Laubach, S.E., 2010. Pure and shear-enhanced compaction bands in Aztec Sandstone. Journal of Structural Geology, in press, doi:10.1016/j.jsg.2010.02.004.

Elata, D., Dvorkin, J., 1996. Pressure sensitivity of cemented granular materials. Mechanics of Materials 23, 147–154.

Elliott, W.C., Aronson, J.L., 1993. The timing and extent of illite formation in Ordovician K-bentonites at the Cincinnati Arch, the Nashville Dome and northeastern Illinois basin. Basin Research 5 (2), 125–135.

Folk, R.L., 1980. Petrology of Sedimentary Rocks. Hemphill Publishing Company, Austin, Texas, pp. 182.

Froelich, A.J., Tazelaar, J.F., 1973. Geologic map of the Balkan Quadrangle, Bell and Harlan Counties, Kentucky. In: Geologic Quandrangle Maps of the United States. U.S. Geological Survey, Kentucky Geological Survey, Washington, D.C. GQ-1127.

Froelich, A.J., Tazelaar, J.F., 1974. Geologic map of the Pineville Quadrangle, Bell and Knox Counties, Kentucky. In: Geologic Quandrangle Maps of the United States. U.S. Geological Survey, Kentucky Geological Survey, Washington, D.C. GQ-1129.

Froelich, A.J., 1972. Geologic map of the Wallin Creek Quadrangle, Harlan and Bell Counties, Kentucky. In: Geologic Quandrangle Maps of the United States. U.S. Geological Survey, Kentucky Geological Survey, Washington, D.C. GQ-1016.

Fu, L., Milliken, K.L., Sharp Jr., J.M., 1994. Porosity and permeability variations in fractured and liesegang-banded Breathitt sandstones (Middle Pennsylvanian), eastern Kentucky: diagenetic controls and implications for modeling dual-porosity systems. Journal of Hydrology 154, 351–381.

Galloway, W.E., Ganey-Curry, P.E., Li, X., Buffler, R.T., 2000. Cenozoic depositional history of the Gulf of Mexico basin. American Association of Petroleum Geologists Bulletin 84, 1743–1774.

Galloway, W.E., 2005. Gulf of Mexico basin depositional record of Cenozoic North American drainage basin evolution. In: Blum, M.D., Marriott, S.B., Leclair, S.F. (Eds.), Fluvial Sedimentology VII, vol. 35. Oxford International, Blackwell, pp. 409–423.

Greb, S.F., Chesnut Jr., D.R., 1996. Lower and lower Middle Pennsylvanian fluvial to estuarine deposition, central Appalachian Basin; effects of eustasy, tectonics, and climate. Geological Society of America Bulletin 108, 303–317.

Hatcher, R.D., Odom, A.L., 1980. Timing of thrusting in the southern Appalachians, USA: model for orogeny? Journal of the Geological Society of London 137, 321–327.

Heald, M.T., Larese, R.E., 1974. Influence of coatings on quartz cementation. Journal of Sedimentary Petrology 44, 1269–1274.

Heald, M.T., Renton, J.J., 1966. Experimental study of sandstone cementation. Journal of Sedimentary Petrology 36, 977–991.

Hower, J.C., Rimmer, S.M., 1991. Coal rank trends in the central Appalachian coalfield. Organic Geochemistry 17, 161–173.

Johnsson, M.J., 1986. Distribution of maximum burial temperatures across northern Appalachian Basin and implications for Carboniferous sedimentation patterns. Geology 14, 384–387.

Lander, R.H., Walderhaug, O., 1999. Predicting porosity through simulating sandstone compaction and quartz cementation. American Association of Petroleum Geologists Bulletin 83, 433–449.

Lander, R.H., Larese, R.H., Bonnell, L.M., 2008. Toward more accurate quartz cement models: the importance of euhedral versus noneuhedral growth rates. American Association Petroleum Geologists Bulletin 92, 1537–1563.

Laubach, S.E., Diaz-Tushman, K., 2009. Laurentian palaeostress trajectories and ephemeral fracture permeability, Cambrian Eriboll Formation sandstones west of the Moine thrust zone, NW Scotland. Journal of the Geological Society of London 166, 349–362.

Laubach, S.E., Milliken, K.L., 1996. New fracture characterization techniques for siliciclastic rocks. In: Aubertin, M., Hassani, F., Mitri, H. (Eds.), Second North American Rock Mechanics Symposium. Balkema, pp. 1209–1213.

Laubach, S.E., Ward, M.E., 2006. Diagenesis in porosity evolution of opening-mode fractures, Middle Triassic to Lower Jurassic La Boca Formation, NE Mexico. Tectonophysics 419, 75–97.

Laubach, S.E., Reed, R.M., Olson, J.E., Lander, R.H., Bonnell, L.M., 2004. Co-evolution of crack-seal texture and fracture porosity in sedimentary rocks: cathodoluminescence observations of regional fractures. Journal of Structural Geology 26, 967–982.

Laubach, S.E., 1988. Subsurface fractures and their relation to stress history in East Texas Basin sandstone. Tectonophysics 156, 495–503.

Makowitz, A., Milliken, K.L., 2003. Quantification of brittle deformation in burial compaction, Frio and Mt. Simon sandstones. Journal of Sedimentary Research 73, 999–1013.

Makowitz, A., Sibley, D.F., 2001. Crystal growth mechanisms of quartz overgrowths in a Cambrian quartz arenite.. In: Journal of Sedimentary Research, 71, pp. 809–816.

Makowitz, A., Lander, R.H., Milliken, K.L., 2006. Diagenetic modeling to assess the relative timing of quartz cementation and brittle grain processes during compaction. American Association of Petroleum Geologists Bulletin 90, 873–885.

Makowitz, A., 2004. The Genetic Association Between Brittle Deformation and Quartz Cementation: Examples from Burial Compaction and Catalysis. Unpublished Dissertation Thesis. The University of Texas at Austin.

McBride, E.F., Diggs, T.N., Wilson, J.C., 1991. Compaction of Wilcox and Carrizo sandstones (Paleocene-Eocene) to 4420 m, Texas Gulf Coast. Journal of Sedimentary Petrology 61, 73–85.

Miller, J.D., Kent, D.V., 1988. Regional trends in the timing of Alleghanian remagnetization in the Appalachians. Geology 16 (7), 588–591.

Miller, R.L., 1962. The Pine Mountain overthrust at the northeast end of the Powell Valley Anticline, Virginia. U.S. Geological Survey. Professional Paper, D69–d72.

Milliken, K.L., Reed, R.M., Laubach, S.E., 2005. Quantifying compaction and cementation in deformation bands in porous sandstones. In: AAPG Memoir 85. American Association of Petroleum Geologists, Tulsa, OK, United States, pp. 237–249.

Milliken, K.L., 1998. Carbonate diagenesis in non-marine foreland sandstones at the western edge of the Alleghanian overthrust belt, southern Appalachians. Special Publication. In: Morad, S. (Ed.), Carbonate Cementation in Sandstones. Distribution Patterns and Geochemical Evolution, vol. 26. International Association of Sedimentologists, pp. 87–105.

Milliken, K.L., 2001. Diagenetic heterogeneity in sandstone at the outcrop scale, Breathitt Formation (Pennsylvanian), eastern Kentucky. American Association of Petroleum Geologists Bulletin 85, 795–815.

Milliken, K.L., 2002. Microscale distribution of kaolinite in Breathitt Formation sandstones (middle Pennsylvanian): Implications for mass balance. Special Publication. In: Worden, R., Morad, S. (Eds.), Clay Cements in Sandstones, vol. 34. Blackwell Science, pp. 335–352.

Milliken, K.L., 2003. Microscale distribution of kaolinite in Breathitt Formation sandstones (middle Pennsylvanian): implications for mass balance. Special Publication. In: Worden, R., Morad, S. (Eds.), Clay Cements in Sandstones, vol. 34. Blackwell Science, pp. 335–352.

Mitra, S., 1988. Three-dimensional geometry and kinematic evolution of the Pine Mountain thrust system, Southern Appalachians. Geological Society of America Bulletin 100, 72–95.

O'Hara, K., Hower, J.C., Rimmer, S.M., 1990. Constraints on the emplacement and uplift history of the Pine Mountain thrust sheet, eastern Kentucky. Evidence from coal rank trends. Journal of Geology 98, 43–51.

Olson, J.E., Laubach, S.E., Lander, R.H., 2007. Combining diagenesis and mechanics to quantify fracture aperture distributions and fracture pattern permeability. In: Geological Society Special Publications, vol. 270, pp. 101–116.

Olson, J.E., Laubach, S.E., Lander, R.H., 2009. Natural fracture characterization in tight gas sandstones: integrating mechanics and diagenesis. AAPG Bulletin 93 (11), 1535–1549.

Paxton, S.T., Szabo, J.O., Adjukiewicz, J.M., Klimentidis, R.E., 2002. Contstruction of an intergranular volume compaction curve for evaluating and predicting compaction and porosity loss in rigid-grain sandstone reservoirs. American Association of Petroleum Geologists Bulletin 86, 2047–2068.

Perez, R.J., Boles, J.R., 2005. An emipirically derived kinetic model for albitization of detrital feldspar. American Journal of Science 305, 312–343.

Poag, C.W., Sevon, W.D., 1989. A record of Appalachian denudation in post-rift Mesozoic and Cenozoic sedimentary deposits of the U.S. middle Atlantic continental margin. Geomorphology 2, 119–157.

Poag, C.W., 1992. U.S. Middle Atlantic continental rise; provenance, dispersal, and deposition of Jurassic to Quaternary sediments. In: Poag, C.W., de Graciansky, P.C. (Eds.), Geologic Evolution of Atlantic Continental Rises. Van Nostrand Reinhold, New York.

Quinlan, G.M., Beaumont, C., 1984. Appalachian thrusting, lithosphere flexure, and the Paleozoic stratigraphy of the eastern interior of North America. Canadian Journal of Earth Science 21, 973–996.

Roden, M.K., Elliott, W.C., Aronson, J.L., Miller, D.S., 1993. A comparison of fission-track ages of apatite and zircon to the K/Ar ages of illite-smectite (I/S) from Ordovician K-bentonites, southern Appalachian Basin. Journal of Geology 101, 633–641.

Roden, M.K., 1990. Apatite-fission track thermochronology of the southern Appalachian Basin: Maryland, West Virginia, and Virginia. Journal of Geology 99, 41–53.

Rowan, E.L., Ryder, R.T., Repetski, J.E., Trippi, M.H. and Ruppert, L.F. 2004. Initial burial results of a 2D burial/thermal history model, Central Appalachian Basin, Ohio and West Virginia. In: USGS Open File Report, Washington, D.C., p. 35.

Secor, D.T.J., Snoke, A.W., Bramlett, K.W., Costello, O.P., Kimbrell, O.P., 1986. Character of the Alleghanian orogeny in the southern Appalachians: part I. Alleghanian deformation in the eastern Piedmont of South Carolina. Geological Society of American Bulletin 97, 1319–1328.

Sippel, R.F., 1968. Sandstone petrology, evidence from luminescence petrography. Journal of Sedimentary Petrology 38, 530–554.

Stamatakos, J., Hirt, A.M., Lowrie, W., 1996. The age and timing of folding in the central Appalachians from paleomagnetic results. Geological Society of American Bulletin 108, 815–829.

Tankard, A.J., 1986. Depositional response to foreland deformation in the Carboniferous of eastern Kentucky. American Association of Petroleum Geologists Bulletin 70, 853–868.

Walderhaug, O., Lander, R.H., Bjørkum, P.A., Oelkers, E.H., Bjørlykke, K., Nadeau, P., 2000. Modelling quartz cementation and porosity in reservoir sandstones: examples from the Norwegian continental shelf. Special Publication. In: Worden, R.H., Morad, S. (Eds.), Quartz Cementation in Sandstones, vol. 29. International Association of Sedimentologists, pp. 39–49.

Walderhaug, O., 1994a. Precipitation rates for quartz cements in sandstones determined by fluid inclusion microthermometry and temperature-history modelling. Journal of Sedimentary Research 64, 324–333.

Walderhaug, O., 1994b. Temperatures of quartz cementation in Jurassic sandstones from the Norwegian continental shelf—evidence from fluid inclusions. Journal of Sedimentary Petrology 64, 311–323.

Walderhaug, O., 1996. Kinetic modeling of quartz cementation and porosity loss in deeply buried sandstone reservoirs. American Association of Petroleum Geologists Bulletin 80, 731–745.

Walderhaug, O., 2000. Modeling quartz cementation and porosity in Middle Jurassic Brent Group sandstones of the Kvitebjørn Field, northern North Sea. American Association of Petroleum Geologists Bulletin 84, 1325–1339.

Wilson Jr., C.W., Stearns, R.G., 1958. Structure of the Cumberland Plateau, Tennessee. Geological Society of America Bulletin 69, 1283–1296.

Zafar, J.S., Wilson, E.N., 1978. The effects of Pine Mountain overthrust and other regional faults on the stratigraphy and gas occurrence of Devonian shales south and east of Big Sandy gas field in Kentucky and Virginia. In: Second Eastern gas shales symposium. U.S. Department of Energy, Morgantown Energy Technology Center, Morgantown, WV, United States, pp. 404–414.

Zang, A., Wong, T.-F., 1995. Effective stiffness and stress concentration in cemented granular material. International Journal of Rock Mechanics and Mining Science.